Efficiency Modeling of Class-E Power Oscillators for Wireless Energy Transfer

R.L.O. Pinto
CTI Design House
Campinas-SP, Brazil
rodrigo.pinto@cti.gov.br

R.M. Duarte, F.R. Sousa
Electrical Engineering Department
UFSC, Florian'opolis-SC, Brazil
rangel@ieee.org

I. Muller, V.J. Brusamarello
Electrical Engineering Department
UFRGS, Porto Alegre-RS, Brazil
ivan.muller@ufrgs.br

***Abstract*—Wireless energy transfer is employed in different applications such as recharging of electrical car battery, implanted biosystems and wireless sensor network nodes. In these applications, the efficiency in the energy transfer process is a key issue, requiring careful design and correct device, circuit and system modeling. In this paper, we present accurate expressions for efficiency calculation of class-E power oscillators targeting an inductive link for wireless energy powering. The model includes the influence of the load resistance variations due to changes on the magnetic coupling between the coils of the link. Moreover, we compare the results obtained from the developed model with those obtained from simulation and measurement of a class-E power oscillator operating at 125 kHz.**

I. Introduction

Wireless power or contactless energy transfer concerns the transmission of electrical energy from an electrical power source to a load without the need of wires. Magnetically coupled coils have been widely used in applications requiring wireless power such as biomedical implanted devices [1], [2], [3], instrumentation systems [4], among others [5], [6]. In such applications, the power transfer from the source to the load is performed by using coils without a magnetic core.

Currently, low power devices are used in important applications such as wireless sensor networks (WSN). Wireless sensor nodes are usually resource constrained platforms, driven by batteries, which limits their energy budget. Additionally, these sensor nodes are often deployed in areas that are difficult to be accessed and can even be mechanically sealed, thus making virtually impracticable the replacement of such energy resources. A feasible solution to this problem is to use an inductive link with the secondary coil positioned in the node and the primary coil in a power device for recharging the device's battery. This approach has been tested in a wireless sensor node developed by the authors called Namimote [7], a low cost and multi-purpose sensor node platform for wireless sensor networks [8].

Efficiency, though, is still a challenging issue in a wireless power system since the energy losses in the overall process can seriously limit any implanted device operation. Moreover, the excitation source has an important role, as its output resistance is a critical parameter. In such context class-E power oscillators citeIslam can be used to generate an excitation signal for wireless energy transfer systems based on inductive links, since it can provide high energy transfer efficiency.

In this paper, we report a model for the efficiency of a class-E oscillator, which accounts for the losses in all passive components, as well as for the dependence on the system load variations reflected in the primary side of the inductive link. The developed model is compared to simulation and measurement results yielding very close values of efficiency for a wide range of load values.

II. Wireless Energy Transfer System

Figure 1 shows a general block diagram of a wireless energy transfer system. We can divide it in three parts: the DC-AC converter, the inductive link and the load. The DC-AC converter is usually composed of an oscillator and a power amplifier, which should be very efficient. The inductive link is an air core transformer composed of inductors L_0 and L_L, connected to the DC-AC converter and to the load through impedance matching networks. The load is commonly a rectifier followed by a voltage regulator and the load itself.

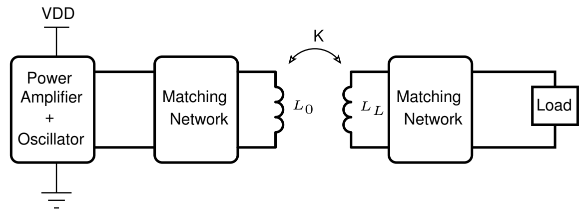

Fig. 1. Block diagram of a wireless power transfer systems.

Most of the works reporting the efficiency of inductive links ignore the energy used to drive the power amplifier, which when accounted for, can considerably degrade the whole system efficiency. In this work, we adopt the solution of merging the signal generator and the driver with the power amplifier in a single circuit, so called a power oscillator. Since the class-E power amplifier topology is recognized for its high efficiency, we keep it as the core of circuit designed.

A. Class-E Power Amplifier

The class-E amplifier belongs to the category of switched amplifiers and is loaded with a high-order reactive network, providing enough degrees of freedom to adapt the switch voltage to have both zero value and zero slope at switch turn-on, which helps to decrease the losses. A schematic diagram of a typical class-E amplifier is depicted in Figure 2. The switch is implemented by the MOS transistor and the reactive load is formed by parallel equivalent of capacitors C_2, inductor L_2 and the resonant circuit formed by the series association

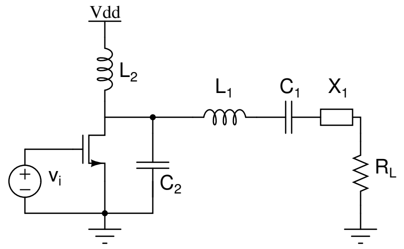

Fig. 2. Schematic diagram of a typical class-E amplifier

between capacitor C_1, inductor $L1$, and the load impedance formed by X_1 and R_L. X_1 can be either inductive of capacitive and represents the resonance frequency mistuning of the series RLC filter. The literature concerning the class-E amplifier is very abundant and evaluating the topic in details is out of the scope of this work [9].

B. Class-E Power Oscillator

Even though the class-E amplifier can work under very high efficiencies, it still requires a driver which should degrade the whole system efficiency. As previously mentioned, we adopted the solution of transforming the class-E amplifier into a self driven amplifier. In order to accomplish it, we provided a positive feedback path between the drain and the gate of the switch transistor by means of C_3 and L_3, as one can notice in the schematic diagram of the class-E oscillator shown in Figure 3.

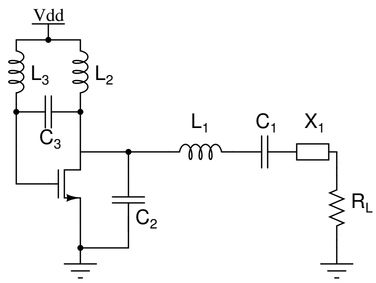

Fig. 3. Schematic diagram of the class-E oscillator

C. Class-E Power Oscillator loaded by the inductive Link

By loading the circuit of Figure 3 with an inductive link we complete the whole wireless energy transfer system as shown in Figure 4. The energy is transmitted to the load R_L through the coupling between L_0 and L_L, whose intensity is given by the coupling factor k.

The impedance of the secondary side strongly influences the behavior of the class-E oscillator, both by changing the oscillation frequency and the circuit efficiency. The latter is strongly influenced by the real part of the impedance of the secondary side reflected on the primary side of the link, R_{Load}, which can be calculated by:

$$R_{Load} = \Re e \left[R_0 + jwL_0 + \frac{w^2 M^2}{jwL_L R_L + Z_L} \right], \quad (1)$$

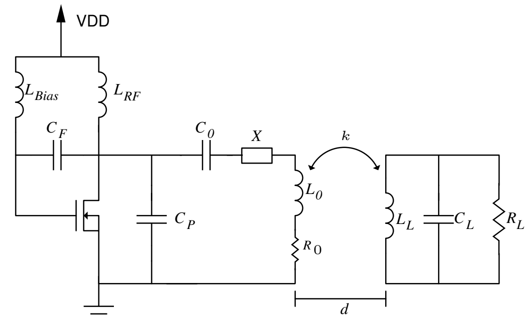

Fig. 4. Schematic diagram of an inductive link circuit used for power transferring

where R_0 represents the equivalent series resistance of L_0 and C_0, Z_L is the parallel equivalent between C_L and R_L and M is related to k according to:

$$M = k\sqrt{L_0 L_L} \quad (2)$$

Hence, the correct estimation of the circuit efficiency dependence on the load variations allows us to devise a structure to adjust the system to operate at the best efficiency point.

III. Efficiency Modelling

In this section, we model the efficiency of the power oscillator of Figure 4, taking into consideration the influence of the reflected load in the primary.

A. Power Transfer Fundamentals

Power transfer is classically analyzed based on a Thevenin model of the energy source, as depicted in Figure 5(a). Depending on the nature of the energy source, alternative models should be envisaged in order to correctly represent the energy supply, such as those illustrated in Figures 5 (b) and (c). In the case studied in this paper, the power oscillator efficiency is better understood if it is modeled as a voltage source in parallel with a resistance connected to the load through a series resistance as inFigure 5(c).

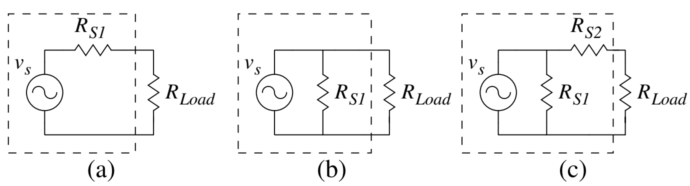

Fig. 5. Power transfer basic circuits

Defining efficiency as the ratio between the power dissipated on the load and the power delivered by the voltage source, we can calculate the efficiency of the circuit of Figure 5(c) as:

$$\eta = \frac{R_{Load} R_{S2}}{(R_{S1} + R_{Load})(R_{S1} + R_{S2} + R_{Load})}, \quad (3)$$

that can be rewritten as below if both source resistances are considered equal to R_{S1}:

$$\eta = \frac{\frac{R_{S1}}{R_{Load}}}{(1+\frac{R_{S1}}{R_{Load}})(1+2\frac{R_{S1}}{R_{Load}})}, \quad (4)$$

From (4), we identify a point of maximum efficiency with respect to the ratio between the source and load impedances. In this specific case, this peak occurs when $\frac{R_{S1}}{R_{Load}} \approx 0.7$, which corresponds to $\eta \approx 17\%$. In Figure 6, the efficiency of the circuits shown in Figure 5 are plotted against the source impedance normalized to the load.

In the energy source based on a class-E power oscillator, the efficiency dependence on the load value has a behavior similar to that of circuit (c), as it will become clear later in this paper.

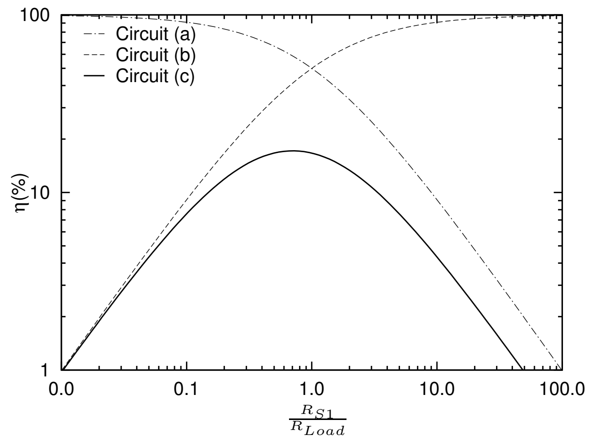

Fig. 6. Efficiency for each circuit of Figure 5.

B. Class-E voltage approximations

Considering a class-E amplifier operating at the optimum point [9], we can approximate the drain voltage waveform as a half-wave sinusoidal, defined as:

$$v_d(t) = \begin{cases} A_d sin(w_0 t) & \text{for } 0 < w_0 t < \pi \\ 0 & \text{for } \pi < w_0 t < 2\pi \end{cases}$$

In order to develop the model proposed in this paper, it is enough to consider a three-term truncated version of the Fourier series of the half-wave sinusoidal given by:

$$v_d(t) = A_d \left[\frac{1}{\pi} + \frac{sin(w_0 t)}{2} - \frac{2cos(2w_0 t)}{3\pi}\right], \quad (5)$$

where A_d is the amplitude of the half wave.

Based on these assumptions, we can model the class-E power oscillator as the circuit depicted in Figure 7, which contains a voltage generator feeding three passive networks: a pi-network formed by L_{RF}, C_F and L_{Bias} (feedback network), the capacitor C_P, enabling high drain efficiency, and the series RLC circuit that is the amplifier load. Differently from the typical class-E amplifier, in which the gate signal is commonly a square voltage, the power oscillator switch is controlled by a sinusoidal voltage. The losses of the passive components are accounted for in the resistors connected in parallel to each passive component.

In the model, the voltages v_g and v_l are sinusoidal waves in the frequency w_0 according to:

$$v_g(t) = -A_g sin(w_0 t) \quad (6)$$

$$v_l(t) = A_l sin(w_0 t) \quad (7)$$

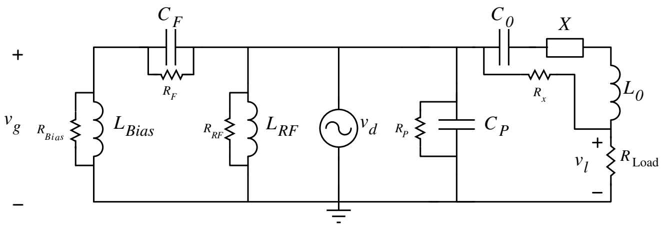

Fig. 7. Class-E power oscillator AC lossy model.

C. Relationship between the amplitudes

The amplitudes A_g and A_l are functions of A_d according to:

$$A_g = K_g A_d \quad (8)$$

$$A_l = K_l A_d \quad (9)$$

Kg is associated to the transfer function of the feedback filter connected between v_d and v_g, which can be computed as:

$$K_g = \frac{1}{2}\sqrt{\frac{(w^2 C_F)^2 + \left(\frac{w}{R_F}\right)^2}{\left(\frac{1}{L_{Bias}} - w^2 C_F\right)^2 + \left(\frac{w}{R_{Bias}} + \frac{w}{R_F}\right)^2}} \quad (10)$$

In order to obtain K_l, we use the transfer function of the RLC series filter, which is illustrated in Figure 6, in which R_{xs} is the series equivalent loss of load filter.

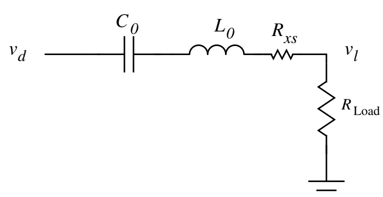

Fig. 8. v_l/v_d bandpass circuit

We then find K_l that is also related only to the fundamental component of the drain voltage, whose basic expression for the absolute value is given by:

$$K_l = \frac{\frac{1}{2}\left(\frac{R_{Load}}{R_{Load}+R_{XS}}\right)}{\sqrt{1+\left(\frac{w_0 L_0}{R_{Load}+R_{XS}} - \frac{1}{w_0 C_0 (R_{Load}+R_{XS})}\right)^2}} \quad (11)$$

The oscillation frequency also depends on the value of R_{Load}, so, the value of K_l can be misestimated if a correction on the oscillation frequency is not performed. The corrected frequency is given by [10]:

$$w = \sqrt{\frac{1}{C_F(L_{Bias} + L_{RF})} - w_{Loss}^2}, \tag{12}$$

where w_{Loss} represents the oscillation frequency deviation, and is given by:

$$w_{Loss}^2 = \frac{R_{Load} C_F R_{BiasS}^2 + L_{RF} R_{BiasS}}{R_{Load} C_F L_{Bias}(L_{Bias} + L_{RF})} \tag{13}$$

D. Losses in the Power Oscillator

Based on the model for the node voltages developed in the previous sections, we have the voltage drop on each device, that are modeled as a parallel combination of a reactive device and an associated loss (see Figure 7). Consequently, the power dissipated can be directly estimated. By taking the root mean square of the voltages drop based on (5), (6) and (7), and referring all the amplitudes to A_d according to expressions (8) and (9), we find the power of each device, as:

$$P_{Bias} = \frac{A_d^2}{R_{Bias}} \frac{K_g^2}{2} \tag{14}$$

$$P_L = \frac{A_d^2}{R_{Load}} \frac{K_l^2}{2} \tag{15}$$

$$P_P = \frac{A_d^2}{R_P} \left[\frac{1}{\pi^2} + \frac{1}{8} + \frac{2}{9\pi^2} \right] \tag{16}$$

$$P_{RF} = \frac{A_d^2}{R_{RF}} \left[\frac{1}{\pi^2} + \frac{1}{8} + \frac{2}{9\pi^2} \right] \tag{17}$$

$$P_F = \frac{A_d^2}{R_F} \left[\frac{1}{\pi^2} + \frac{1}{2} \left[K_g^2 + K_g + \frac{1}{4} \right] + \frac{2}{9\pi^2} \right] \tag{18}$$

$$P_x = \frac{A_d^2}{R_X} \left[\frac{1}{\pi^2} + \frac{1}{2} \left[K_l^2 - K_l + \frac{1}{4} \right] + \frac{2}{9\pi^2} \right] \tag{19}$$

E. Class-E Power Oscillator Efficiency

The oscillator efficiency is defined as the power delivered to the load divided by the power loss in all components:

$$\eta = \frac{P_L}{P_{Bias} + P_{RF} + P_P + P_F + P_X + P_L} \tag{20}$$

By applying (14) to (19) into (20), we obtain (21), which is the complete expression for the oscillator efficiency.

IV. RESULTS

We validated the model presented here based on ADS simulations and measurements performed in a circuit similar to that brought in Figure 3. It uses a MOSFET IRL540ns and the components for the power oscillator given in Table I.

TABLE I. VALUES OF THE CIRCUIT PARAMETERS

L_{RF}	5.86 μH	C_F	45.3 nF
L_{Bias}	25.56 μH	C_P	96,9 nF
C_0	22.8 nF	L_0	71.87 μH
R_F	5.6 kΩ	R_{Bias}	25.56 kΩ
R_{RF}	118 Ω	R_P	2.17 kΩ

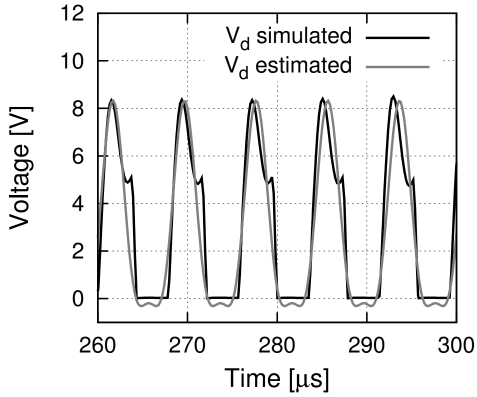

Fig. 9. Plot of estimated and simulated drain voltage waveform.

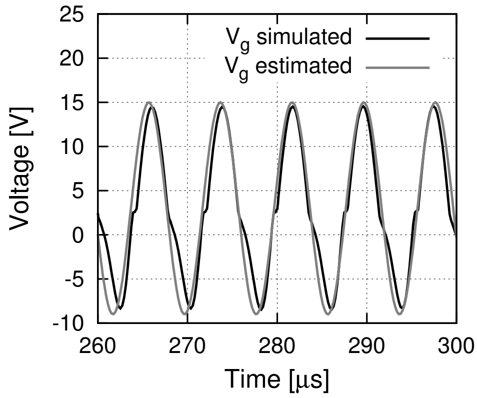

Fig. 10. Plot of estimated and simulated gate voltage waveform.

The voltages on the drain and on the gate terminals of the transistor obtained by simulations as well as estimated by (5) and (6) are plotted in Figures 9 and 10 respectively. In both cases the simulations are quite close to the proposed expressions.

Finally, Figure 11 shows the calculated efficiency using (21) compared to the efficiency obtained from simulation and measurement results as well as the efficiency calculated with the model of [11]. Our model fits better with measurement and simulation in the range of the optimal load, which extends from 5 Ω to 20 Ω. For low values of R_{Load}, the discrepancies are high and are mainly due to the switch losses which were not taken into account. These results allow us to envisage a system to track the maximum efficiency by adjusting a few parameters of the circuit.

$$\eta = \frac{\frac{1}{2}\left[\frac{K_l^2}{R_{Load}}\right]}{\frac{1}{2}\left[\frac{K_g^2}{R_{Bias}} + \frac{K_l^2}{R_{Load}}\right] + \left[\frac{1}{\pi^2} + \frac{1}{8} + \frac{2}{9\pi^2}\right]\left[\frac{1}{R_P} + \frac{1}{R_{RF}} + \frac{1}{R_F} + \frac{1}{R_X}\right] + \frac{1}{2R_F}\left[K_g^2 + K_g\right] + \frac{1}{2R_X}\left[K_l^2 - K_l\right]} \quad (21)$$

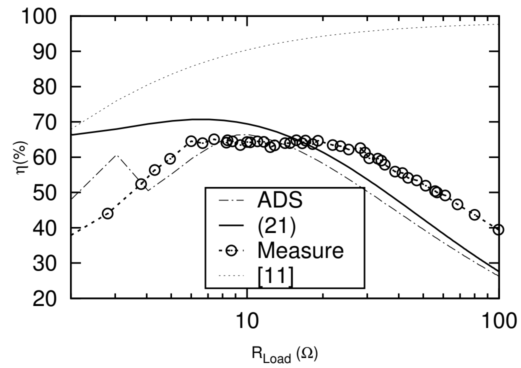

Fig. 11. Efficiency of the simulated and measured Class-E oscillator as function of the load values

V. Conclusion

In this paper, we analyzed the efficiency of a class-E power oscillator, considering the influence of the load variations. The model developed was validated by comparing its outcomes with results obtained from measurements and simulations of a class-E power oscillator circuit. In addition, it was shown that the class-E oscillator efficiency presents a maximum peak for a given optimum R_{Load}. Our equation presented an accurate method for obtaining the optimum load resistance, which can be useful for optimum efficiency locking in wireless energy transfer systems.

Acknowledgment

The authors would like to thank CNPq and INCT NAMITEC for the partial financial support.

References

[1] P. Li and R. Bashirullah A wireless power interface for rechargeable battery operated medical implants. In *IEEE Trans. Circuits Syst. II, Exp. Briefs*, vol. 54, no. 10, pp. 912916, Oct. 2007.

[2] R.R. Harrison Designing efficient inductive power links for implantable devices, In *In: Proc. 2007 IEEE Intl. Symposium on Circuits and Systems (ISCAS 2007), New Orleans, LA*, pp. 2080-2083, 2007.

[3] Q. Ma, M. Haider, S. Yuan, and S. Islam. Power-oscillator based high efficiency inductive power-link for transcutaneous power transmission. In *Circuits and Systems (MWSCAS), 2010 53rd IEEE International Midwest Symposium on*, pages 537 –540, Aug. 2010.

[4] J. Boeij, E. Lomonova, J.L. Duarte, and A.J.A. Vandenput Contactless power supply for moving sensors and actuators in highprecision mechatronic systems with long-stroke power transfer capability in x-y plane, In *Sens. Actuators A, Phys.*, vol. 148, no. 1, pp. 319328, Nov. 2008.

[5] C.G. Kim, D.H. Seo, J.S. You, J.H. Park, B.H. Cho Design of a Contactless Battery Charger for Cellular Phone, In *IEEE Transactions on Industrial Electronics*, Vol. 48, N. 6, pp. 1238-1247, 2001.

[6] T. Bieler, M. Perrottet, V. Nguyen, and Y. Perriard, Contactless power and information transmission, In *Conf. Rec. IEEE-IAS Annu. Meeting*, vol. 1, 2001, pp. 8388.

[7] I. Muller, E.P. Freitas, A.A. Susin, C. Pereira, Namimote: A Low Cost Sensor Node for Wireless Sensor Network. In *Sergey Andreev, Sergey Balandin, Yevgeni Koucheryavy. (Org.). Internet of Things, Smart Spaces, and Next Generation Networks. Internet of Things, Smart Spaces, and Next Generation Networks*, 1ed.Berlin: Springer, 2012, v. 1, p. 391-400.

[8] V.J. Brusamarello, Y.B.Blauth, R. Azambuja, I. Muller, F.R. Sousa, Power Transfer with an Inductive Link and Wireless Tuning, In *IEEE Transactions on Instrumentation and Measurement*, 2013, to be published.

[9] N. Sokal and A. Sokal. Class e-a new class of high-efficiency tuned single-ended switching power amplifiers. *Solid-State Circuits, IEEE Journal of*, 10(3):168 – 176, June 1975.

[10] J.W.M. Rogers, C. Plett Radio Frequency Integrated Circuit Design. In *ARTECH HOUSE*, 2003.

[11] M.K. Kazimierczuk. RF Power Amplifiers. *Wiley*, November 2008.